The hydration of formic acid and acetic acid

Stefano Soffientini, Leonardo Bernasconi and Silvia Imberti

Published version information

Citation: Soffientini, S, L Bernasconi, and S Imberti. "The hydration of formic acid and acetic acid." Journal of Molecular Liquids, vol. 205 (2015): 85-92.

doi: 10.1016/j.molliq.2014.11.030

The hydration of formic and acetic acid

Stefano Soffientini

Università degli Studi di Milano-Bicocca, Dipartimento di Fisica, Milano, Italy.

Leonardo Bernasconi and Silvia Imberti[1]

STFC, Rutherford Appleton Laboratory, Harwell Oxford Campus, OX11 0QX, United Kingdom.

Abstract

Formic and acetic acid share the unique feature, among carboxylic acids, of crystallising in the form of long chains, containing both O-H$\cdots$O and C-H$\cdots$O hydrogen bonds. We have performed a neutron diffraction study of the pure acids and of three mixtures of acid and water (2:1, 1:1 and 1:2). The data from the SANDALS diffractometer at ISIS have been modelled using the Empirical Potential Structure Refinement code, which is able to reproduce a set of configurations compatible with the experimental data. The relative importance of the hydrogen bonds present in the solution is assessed based on geometrical criteria: bond length and directionality as well as number of bonds. At all concentrations, the carbonyl oxygen on the carboxylic group is the most active site for strong hydrogen bond. The tendency to establish direct interactions between acid molecules in the presence of water is reduced for acetic acid by a larger degree than for formic acid. The overall tendency is for a greater number of hydrogen bonds being formed when the solution is more diluted. The availability of good quality structural data on the liquid states is of great importance for the understanding of spectroscopic experiments and for benchmarking both classic molecular dynamics and ab initio simulations. The results provide a springboard to more realistic models of aerosol formation, which is greatly needed for better understanding of clouds formation processes.

1. Introduction

Anthropogenic aerosol particles such as sulfate and carbonaceous aerosols can influence climate in several ways: they scatter and absorb solar radiation and thermal radiation from the Earth (direct effects) and they also act as cloud condensation nuclei and ice nuclei (indirect effects). Indirect aerosol effects are nowadays one the greatest sources of uncertainty in assessing the human impact on climate change.[1] While nucleation of sulfate aerosol particles is well

[1]Corresponding author: silvia.imberti@stfc.ac.uk

established, nucleation from organic precursors has not been proven. One currently held hypothesis states that organic mixtures form initially a different phase (glassy or crystalline), then give rise to heterogeneous nucleation. The alternative one is that the process triggered by non-sulfate organic molecules in the atmosphere is not nucleation but rather condensational growth.[2] In either case, a quantitative knowledge of the fundamental nucleation and crystallisation processes of organic-water mixtures is essential in order to understand and predict the impact of organic pollution on the Earth's atmosphere and climate. [3]

Infrared spectra of aqueous formic acid and acetic acid aerosols reveal that their internal structure critically depends on the particle formation conditions (e.g. temperature and humidity variations) and, especially for the solutions, on their composition.[4] But, as stated by Koop et al.[5]:"(...) before these effects are at a point that they can be described for atmospheric purposes, there is still a large lack of basic physical and chemical understanding in these systems, requiring a considerable piece of basic research before significant progress can be made in this area." Indeed, several basic questions remain unanswered, such as: What are the glass-forming properties of the neat acid and of its mixture with water? What is the stability of these complexes when temperature and humidity level vary? How hygroscopic is an acid-water complex? and closer to the point of this article: What is the structure of an acid-water complex in the liquid and glassy state? How does cooperativity affect this geometry when the number of hydrating water molecules increases?

In the present contribution we have performed a neutron diffraction study of three mixtures of acid and water, at approximately 70%, 50% and 30% acid mole fraction. For each concentration three independent patterns of formic acid/water mixture, and four patterns of acetic acid/water mixtures have been measured, with deuterium substituted for hydrogen to a varying degree. For each concentration, the three (or four) patterns have been used to simultaneously drive a Monte Carlo simulation, through the well tested EPSR method[6]. In this way the structural properties have been calculated as an average over an ensemble of simulation boxes, all compatible with the neutron diffraction experimental data.

Formic and acetic acid share the unique feature, among carboxylic acids, of crystallising in the form of long chains, containing both O-H$\cdots$O and C-H$\cdots$O hydrogen bonds; these chains are then bonded to each other via dispersion forces, forming a secondary and tertiary structure.[7] This is at variance with the gaseous state, which is mostly constituted of cyclic dimers.[8] Spectral features of the pure liquids have been measured in the past [9][10], but their interpretation is still somewhat open. This constitutes the focus of many of the ab initio studies on small complexes [11, 12, 13, 14, 15]. Several studies have tackled the structure of both neat acids in the liquid state (see for example Chelli et al.[16] and Imberti et al.[17] and references therein), but data on the aqueous system were still mostly missing (with one notable exception in Ref.[18]).

Our main goal is to extract the radial and angular distribution functions of the water-acid system for each concentration and to compare them with those

of the pure acids[17]. The relative importance of the various hydrogen bonds present in the solution is assessed based on geometrical criteria: bond length and directionality as well as number of bonds.

2. Materials and Methods

The neutron experiments have been performed on the SANDALS diffractometer at the ISIS spallation neutron source, located at the Rutherford Appleton Laboratory (United Kingdom). SANDALS is a total scattering neutron diffractometer optimized for the study of liquids and amorphous samples containing light elements. The physical quantity measured by the diffractometer is the differential scattering cross section $d\Sigma/d\Omega$ as a function of the exchanged wave vector Q (defined as the modulus of the difference between the incident and the scattered neutron wave vectors). Through the basic theory of neutron scattering[19], it is possible to relate this quantity to the static structure factor $F(Q)$, which is the Fourier transform of the atomic pair distribution function $g(r)$. The latter contains the information about the correlation between the positions of two atoms in the system at a given moment.

The ISIS pulsed neutron source produces a time-structured beam with a frequency of 50Hz. The diffractometer faces a liquid methane moderator operating at 110 K, which provides neutrons in the wavelength range between 0.05 and 4.95 Å. The sample is placed in an evacuated chamber after a collimated flight path, 11.02 m from the moderator face. SANDALS works in transmission geometry, the samples are contained in flat TiZr alloy cells (internal thickness and wall thickness 1mm) and these are mounted on an automated sample changer. Each detector on SANDALS provides an independent measure of the structure factor $F(Q)$, within the Q range allowed by its fixed angular position. The wavelength of the detected neutron is determined by its time of flight from the moderator. The instrument has 633 ZnS scintillator detectors covering an angular range between 3.5 and 40 degrees. The forward scattering geometry minimizes the inelasticity corrections that are applied to the data from light element containing samples. The combination of the wide wavelength range and angular coverage provides a very wide Q range, running from 0.2 to 50 Å^{-1}.

The H/D isotopic substitution method [20] has been applied, in order to provide several independent determinations of the structure factor of the acetic acid (a.a.) and formic acid (f.a.) solutions. The samples have been purchased from Sigma-Aldrich. In the case of a multicomponent system, it can be shown[21] that the structure factor extracted from a neutron diffraction experiment is a linear combination of the partial structure factors $S_{\alpha\beta}(Q)$ in the following way:

$$F(Q) = \sum_{\alpha\beta \geq \alpha} (2 - \delta_{\alpha\beta}) c_\alpha c_\beta b_\alpha b_\beta S_{\alpha\beta}(Q) \quad (1)$$

where α and β are two atom types present in the system, $\delta_{\alpha\beta}$ is the Kronecker delta function, c is their concentration and b their scattering length [22]. Since the scattering length b varies from one isotope to another, the shape of the

measured function $F(Q)$ can vary quite dramatically with changing the isotopes involved. In particular, by substituting ^{1}H (b =-3.740 fm) with ^{2}H (b =6.671 fm), it is possible to highlight H-X correlations, where X is a non-substituted atom (e.g. oxygen).

The standard corrections and normalizations have been applied to the data through the set of programs gathered under the graphical interface *GudrunN*. The theoretical background to the operations performed by the program are described in reference [21]. Both *GudrunN* and its X-rays equivalent *GudrunX*[23] have been written by Alan K. Soper (ISIS, STFC) and are described in detail in the manual *GudrunN and GudrunX. Programs for correcting raw neutron and x-ray diffraction data to differential scattering cross section.*[21]

2.1. Data modelling

Models of the experimental data have been constructed using the Empirical Potential Structure Refinement (EPSR) program. The method has been described in detail elsewhere (see Soper[24] and references therein) and therefore only a brief summary will be given here. The algorithm is based on a classical Monte Carlo simulation of the molecular system under study at fixed concentration and density, and employs an iterative algorithm that aims at building an atomistic three dimensional model consistent with the scattering data. The simulation proceeds through a number of stages. In the first stage the simulation follows the standard Monte Carlo algorithm for simulations of molecular structures [19], based on a pairwise reference potential (Lennard-Jones plus Coulomb). In the following stage a perturbation potential is determined from the difference between the calculated and experimental structure factors. The simulation box is equilibrated with the reference plus empirical potential and a new empirical potential is calculated and added to the previous one. This iterative process drives the model into agreement with the data. Once agreement is reached between the experimental and model structure factors, the final stage of the procedure is undertaken and structural information is collected in the form of ensemble averages. Each simulation box contained 2000 molecules. All the simulation details are summarised in table 1.

In principle it is possible to calculate the number of molecules which dissociate in water based on tabulated pKa values, according to the Henderson-Hasselbalch equation. In reality, at the high concentrations studied here, there is a considerable disagreement between calculated and measured pH values. This fact points towards a rich dissociation scenario, which may include the formation of protonated acid molecules and other complexes. For these reasons, the simulations presented here, but in fact mostly only the 0.30 formic acid in water one, can only be a somewhat simplified model of the real system.

Each molecule is obtained as a semi-rigid[24] atomic configuration, defined by geometry, such as bond lengths and angles. The intramolecular structure of these molecules is known and a number of sources in literature carry this information. In this work the intramolecular structure of the acid molecules (detailed in table 2) has been optimized in vacuum using the free computational chemistry software Ghemical 2.0 [25]. It is known that the intramolecular structure

Table 1: Composition (molar fraction of the acid) and density for the formic and acetic acid solutions EPSR simulations. The system density has been calculated as a weighted average. EPSR determines the box size based on the total number of molecules (2000) and on the given solution density.

	formic acid (f.a.)			acetic acid (a.a.)		
Acid molar fraction	0.35	0.55	0.74	0.30	0.50	0.70
Density[$Å^{-3}$]	0.09533	0.09215	0.08897	0.09300	0.08880	0.08510
Molecules no. - acid	707	1109	1474	600	1000	1400
Molecules no. - water	1293	891	526	1400	1000	600

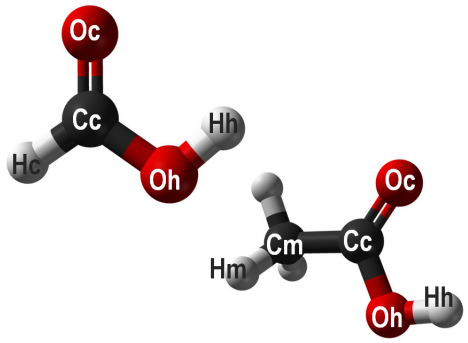

Figure 1: Atom type labelling used for the Lennard-Jones potentials in the EPSR simulation

in vacuum may differ from the one in the bulk liquid, but in the case of the simulations shown in this study, the difference was not appreciable e.g. there was no significant misfit in the high-Q region of the diffraction patterns. For the water molecules, Single Point Charge Extended [26] has been used for both geometry and potentials. A picture of the acid molecules with atom's labelling is included for convenience (Figure 1).

The seeding (*reference*) potentials have been derived from different sources in the literature. For acetic acid Jorgensen's OPLS parametrization [27] has been used; this was originally aimed at the reproduction of thermodynamic properties of liquids, such as density and latent heat of vaporization, but has proven to work well also for structural properties. For formic acid the potential has been obtained from the work by Jedlovszky *et al.* [28, 29]. This potential has been derived specifically for reproducing structural patterns reliably. Both these potentials have been previously tested in an EPSR simulation with success[17]. The actual values used for the potentials are summarized in table 3. All of the EPSR simulations have been run under the same conditions, allowing for a maximum amplitude of the non parametrized empirical potential of about 30 kJ/mol (in addition to the reference potential). The simulations have been equilibrated for at least ∼1500 Monte Carlo cycles (for a total of 10^6 atom moves), and approximately 2500 configurations compatible with the experimental data have been averaged.

Table 2: Bond lengths and angles for the acids molecules and water. Atom labels: in both molecules there are Cc=central carbon, Oc=carbonyl oxygen, Oh=hydroxyl oxygen, Hh=hydroxyl hydrogen; additionally in acetic acid there is Cm=methyl carbon, Hm=methyl hydrogen, in formic acid there is Hc=carbonyl carbon. See also figure 1.

acetic acid		formic acid	
Oh-Hh	0.9498 Å	Oh-Hh	0.9482 Å
Oh-Cc	1.3416 Å	Oh-Cc	1.3265 Å
Cc-Oc	1.2186 Å	Cc-Oc	1.2146 Å
Cm-Hm	1.0999 Å	Cc-Hc	1.0770 Å
Cm-Cc	1.4949 Å	$Oh\widehat{Cc}Hc$	117.67°
$Hm\widehat{Cm}Hm$	109.17°	$Oh\widehat{Cc}Oh$	121.26°
$Cc\widehat{Cm}Hm$	109.79°	$Oc\widehat{Cc}Hc$	120.88°
$Cm\widehat{Cc}Oh$	115.61°	$Cc\widehat{Oh}Hh$	110.64°
$Oh\widehat{Cc}Oc$	122.38°	water	
$Cm\widehat{Cc}Oc$	120.95°	Ow-Hw	0.9760 Å
$Cc\widehat{Oh}Hh$	111.49°	$Hw\widehat{Ow}Hw$	104.50°

Measured and calculated structure factors. For each formic acid concentration 3 independent structure factors have been measured (fully protiated, fully deuteriated and HCOOD in D_2O). For each acetic acid concentration 4 independent structure factors have been measured (fully protiated, fully deuteriated, CH_3COOD in D_2O and CD_3COOH in H_2O). The agreement between the measured data and the calculated structure factors can be inspected in figure 2 for their lowest concentration. The other two concentrations show similar agreement. The original data are available through the ISIS database at https://data.isis.stfc.ac.uk.

Radial distribution functions. Each formic acid solution contains 7 distinct atomic species (5 for the acid molecule, and 2 for the water molecule). Hence we have 28 distinct radial distribution functions $g_{\alpha\beta}(r)$. Similarly, each acetic acid solution contains 8 distinct atomic species (6 for the acid molecule, and 2 for the water molecule), giving a total of 36 radial distribution functions. Amongst these, we will focus our attention primarily on the oxygen-hydrogen distribution functions, for the reason that they provide direct information on the nature of the molecular bonds in our systems. The acid molecules examined in the present work form hydrogen bonds with either other acid molecules or with water molecules, which involve an oxygen atom on one molecule (acceptor) and a oxygen or carbon atom on another molecule (donor).[30] In the solution studied here, the hydrogen atom involved in the intermolecular bond is in turn chemically bonded either to another oxygen atom or to a carbon atom. As a consequence, also the RDFs relative to the oxygen-oxygen and to the carbon-oxygen are very important for the description of the hydrogen bond, and in particular for the characterisation of its directionality. For each concentration a subset of the RDFs has been calculated and illustrated in the following pages, grouped as acid-acid, acid-water and water-water correlations. In the case of

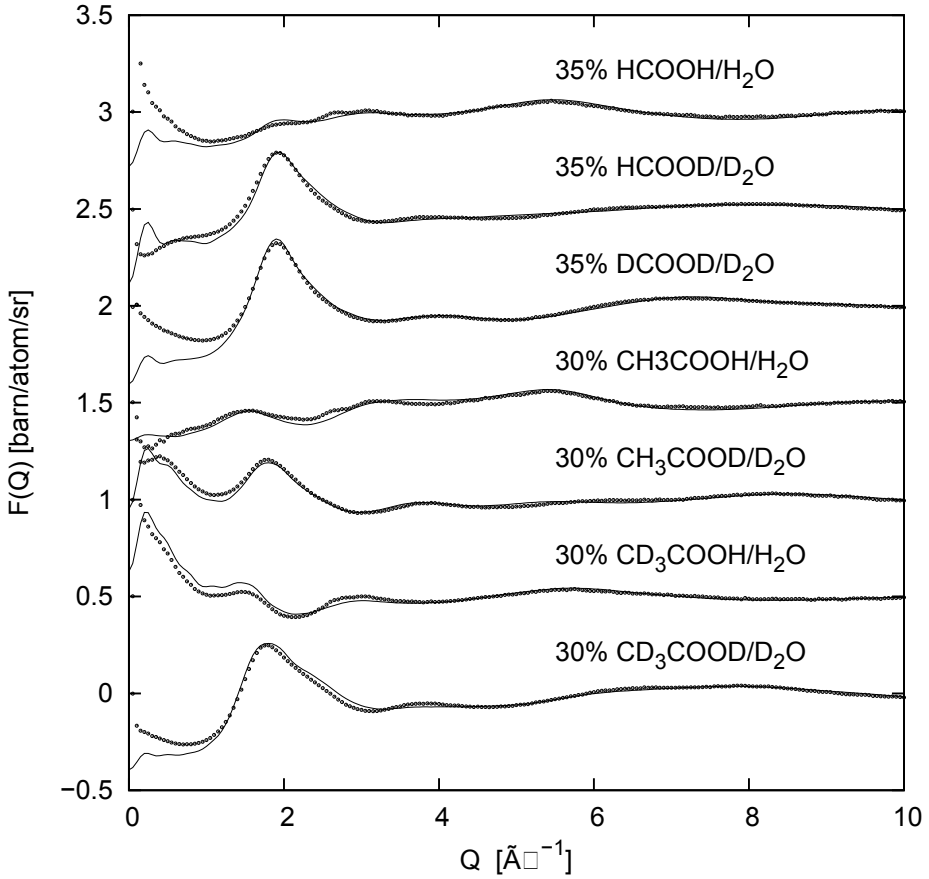

Figure 2: Measured (marks) and calculated (line) structure factors for formic and acetic acid in water at their lowest concentrations.

Table 3: Potential parameters used as a *reference* (seeding) potential for the EPSR simulations. The potential is composed by a Lennard-Jones part, characterised by well depth ϵ and minimum approach σ, plus Coulombic attraction/repulsion, mass m and partial charge q

Atom	ϵ [kJ/mol]	σ [Å]	m [amu]	q [e]
		formic acid		
Hc	0.020	0.80	2	0.1073
Cc	0.376	3.73	12	0.4447
Oc	1.214	2.67	16	−0.4324
Oh	0.392	3.18	16	−0.5530
Hh	0.100	0.99	2	0.4333
		acetic acid		
Cm	0.276	3.50	12	−0.1800
Hm	0.126	2.50	2	0.0600
Cc	0.440	3.75	12	0.5200
Oc	0.879	2.96	16	−0.4400
Oh	0.712	3.00	16	−0.5300
Hh	0.000	0.00	2	0.4500
		water		
Ow	0.650	0.32	16	−0.8476
Hw	0.000	0.00	2	0.4238

acid-acid correlations the results of the solutions have been compared to the ones obtained for neat acids[17].

Coordination numbers. For each pair RDF the corresponding coordination number can been calculated, defined as the number of particles of type β between distances 0 and r_{max} from a particle of type α, and this definition is the one that is adopted operatively within EPSR[6]. This is formally expressed as an integral over the radial distribution function:

$$n_{\alpha\beta}(r) = 4\pi\rho c_\beta \int_0^{r_{max}} r^2 g_{\alpha\beta}(r) dr \tag{2}$$

where ρ is the number density (in atoms/Å^3) of the system and c_β the number fraction of species β. The upper limit of integration r_{max} is usually chosen to correspond to the minimum after the first diffraction peak. The chosen radial limit and the coordination number thus obtained are summarised in table 2. Please note that while $g_{\alpha\beta}(r) = g_{\beta\alpha}(r)$ it is usually the case that $n_{\alpha\beta}(r) \neq n_{\beta\alpha}(r)$. The coordination number is also known as the number of first neighbours and it is useful to note that for a crystalline material this quantity is perfectly determined by the regular distribution of the molecules in the lattice. In the case of amorphous materials, on the contrary, this number has an intrinsic uncertainty, as the disordered structure implies that each molecule has a different number of neighbours. Hence the error on the coordination number is a measure of the disorder and, beyond a certain point, it cannot be reduced by averaging over more configurations.

Angular distributions. Also important to the definition of the strength of a hydrogen bond, is a measure of its directionality, defined by the angle formed by three atoms. Within EPSR, two atoms are defined as bonded if their distance in a given configuration is smaller than a given radius (defined for each atom couple in table 2). The program scans through the box and calculates the bond angle for every triplet of atoms which satisfies the bonding conditions[6]. By averaging over a number of configurations, a smooth angular distribution is generated. The intra-molecular distances have been defined within 10% from the input equilibrium distances (table 2). The inter-molecular distances are not defined *a priori*, but rather they are determined by the intermolecular forces. The radial position of the minimums before and after the first maximum in the relevant RDF are used to define the bond range.

3. Results and Discussion

Acid-acid correlations. In figure 3 the RDFs relative to oxygen-hydrogen bonds between acid molecules are reported, with formic acid as a continuous line and acetic acid as a dashed line. The three concentrations examined in this paper are reported together, for the sake of comparison, with the pure acid results.[17]. The pure acid is the top line of each group of four, followed by 70% and 50%, with 30% (0.7, 0.5 and 0.3 molar) at the bottom.

The most prominent feature in figure 3 is determined by a correlation in the carbonyl oxygen to hydroxyl hydrogen Oc$\cdots$Hh RDF for both acids (more symbols explained in the caption to table 2). The first neighbour peak is in the range from 1.3 Å to 2.5 Å, displaying a peak maximum at 1.75 Å for both acids. The distance of 1.75 Å has been highlighted by a vertical line in this and all of the subsequent RDF pictures in this paper, in order to facilitate comparison among separate plots. The existence of a Oh-Hh$\cdots$Oc bond is supported by the presence of peaks also in the Oh$\cdots$Oc correlation functions, in figure 4. In fact the $g_{Oc\cdots Oh}(r)$ presents a peak at approximately 2.7 Å. The peak position at 2.7 Å has also been highlighted by a second vertical line. This distance is explainable as the sum of the intramolecular Oh-Hh bond (0.95 Å) and the intermolecular Oc$\cdots$Hh bond (1.75 Å) just seen in figure 3. This calculation is clearly implying a linear Oh-Hh$\cdots$Oc bond, as subsequently confirmed by the calculation of the angular distributions (figure 5). The linearity of the Oh-Hh$\cdots$Oc angles, together with the intensity of the peak and the fact that it occurs at a distance comparable (in fact slightly shorter) than the oxygen-hydrogen bond in water, indicates the presence of a strong[30] Oc-Hh bond in these solutions.

In both figure 3 and 4, the peak positions are not appreciably modified by the addition of water at any of the concentrations studied so far, while their intensity varies in the case of acetic acid. In fact, the intensity of an acid-acid correlation peak is expected to increase as we decrease the acid concentration (c_β in equation 2.1) if the number of bonds has to remain constant. In our case the peak intensity either remains constant (f.a.) or decreases (a.a.) by decreasing concentration (e.g. top to bottom), which clearly indicates that the

number of bonds is decreasing, as is also evidenced in figure 9. This picture will be explained in greater detail in the following.

In figure 3 the second notable feature is in the Oh$\cdots$Hh RDF. In the $g_{Oh\cdots Hh}(r)$ the first main peak is at 2.0 Å for formic acid and at 1.85 Å for acetic acid e.g. at a distance compatible with bonding, but it's not very pronounced. The coordination numbers from table 4 suggest that it may be not very frequent. Nevertheless, when present, this bond is close to linear (see figure 5), presumably because of the strong hydroxyl dipole being involved in the bond as in the case of the Oc$\cdots$Hh just seen. Despite the fact that the partial charges on the Oh and Hh atoms are the same in the two acids, the hydroxyl dipole ability to form bonds seems to be stronger in the case of acetic acid than in the case of formic acid, a feature that will be highlighted again in the acid-water correlations.

Finally in figure 3 we also report the RDFs that involve the carbonyl hydrogen Hc for formic acid and the methyl hydrogen Hm for acetic acid. In $g_{Oc\cdots Hc}(r)$ and $g_{Oh\cdots Hc}(r)$ it is not really possible to determine a peak position, but merely a distance of approach that is as low as 2.0 Å. In the RDFs that involve the methyl hydrogen Hm for acetic acid, this distance is pushed further away to approximately 2.5 Å. For this reason in the latter two cases the distance at which the coordination number has been calculated (3.5 Å) has been fixed to the same number for both acids to facilitate the comparison.

Qualitatively the correlation functions that involve only atoms from the carboxylic group are very similar for the two acid molecules. It is worth noting, though, that the acetic acid peak in figures 3 and 4, decays more rapidly with decreasing acid concentration than the formic acid does. This suggests that the tendency to form an acid-acid bond is more disturbed by the presence of water in the acetic acid than it is in the formic acid case. Moreover, in the case of acetic acid the $g_{Oc\cdots Hh}(r)$ shows a second peak that is more pronounced for the solutions than it is in the case of the pure acid, where it is almost completely absent. This may indicate that the influence of water on the ability of the acid molecules to form bonds with each other might also have an effect that goes beyond the first nearest neighbour.

Finally it is worth mentioning that, because of the size of the molecules, the carbon-oxygen RDFs in figure 4 are in effect a centre-of-mass to centre-of-mass correlation.

All of the coordination numbers for acid-acid correlations are collected in table 4. For clarity, the coordinations have also been plotted in figure 9 as a histogram of the coordination number as a function of the acid concentration for both acids. These numbers are usually close to 1 at the highest concentrations, indicating that on average each oxygen only bonds to one hydrogen at a time, and it drops rapidly to less than 1 at the lower concentrations, indicating that this bonding doesn't always occur. It is possible to notice that the acid-acid coordination numbers diminish as the water concentration increases. This may be expected as the water molecules compete with the acid molecules in forming hydrogen bonds, e.g. the acid molecules become more and more hydrated. For the same reason all coordination numbers $n_{\alpha\beta}$ follow the trend of c_β. It is

Table 4: Coordination number and chosen radial limit for its calculation for formic and acetic acid. The coordination number is calculated numerically as the number of atoms β to be found within a certain radius from atom α.

bond	r_{max} [Å]	f.a. 70%	f.a. 50%	f.a. 30%
Oc···Hc	3.5	1.8 ± 1.0	1.6 ± 1.0	1.1 ± 0.9
Hc···Oc	3.5	1.8 ± 0.9	1.6 ± 0.9	1.1 ± 0.9
Oc···Hh	2.5	0.7 ± 0.6	0.5 ± 0.6	0.3 ± 0.5
Hh···Oc	2.5	0.7 ± 0.6	0.5 ± 0.6	0.3 ± 0.5
Oc···Hw	2.5	0.4 ± 0.6	0.7 ± 0.7	1.1 ± 0.8
Hw···Oc	2.5	0.6 ± 0.6	0.4 ± 0.5	0.3 ± 0.5
Oh···Hc	3.5	1.4 ± 0.9	1.2 ± 0.9	0.9 ± 0.8
Hc···Oh	3.5	1.4 ± 0.9	1.2 ± 0.9	0.9 ± 0.8
Oh···Hh	2.5	0.2 ± 0.4	0.2 ± 0.4	0.1 ± 0.3
Hh···Oh	2.5	0.2 ± 0.4	0.2 ± 0.4	0.1 ± 0.3
Oh···Hw	2.4	0.1 ± 0.4	0.3 ± 0.5	0.4 ± 0.5
Hw···Oh	2.4	0.2 ± 0.4	0.2 ± 0.4	0.1 ± 0.3
Ow···Hc	3.5	1.7 ± 1.0	1.4 ± 1.0	1.0 ± 0.9
Hc···Ow	3.5	0.6 ± 0.8	1.1 ± 1.1	1.9 ± 1.2
Ow···Hh	2.5	0.7 ± 0.6	0.6 ± 0.6	0.4 ± 0.5
Hh···Ow	2.5	0.3 ± 0.5	0.4 ± 0.5	0.7 ± 0.5
Ow···Hw	2.4	0.5 ± 0.6	0.8 ± 0.7	1.1 ± 0.7
Hw···Ow	2.4	0.2 ± 0.4	0.4 ± 0.5	0.6 ± 0.5

evident from figure 9 that overall both acid molecules and water molecules have an increase in their total coordination number, when more water molecules are added. It is therefore possible to state that some sort of cooperative effect intervenes in making the samples "stickier", whose quantification is beyond the scope of the present technique. This finding has important consequences for the physical chemistry of aerosol particles.

Acid-water and water-water correlations. In figure 6 the RDFs relative to oxygen-hydrogen bonds between acid molecules and water molecules are reported, with formic acid in a continuous line and acetic acid in a dashed line. The three concentrations examined in this paper are reported together with the Ow···Hw RDF for pure water (dotted line at the bottom of the figure). The 70% concentration is the top line of each group of three lines, followed by 50%, with 30% at the bottom. The most prominent features in this figure are in the Hh···Ow, Ow···Hw and Oc···Hw RDFs, at the top of the picture. Is it important to notice how the carbonyl oxygen Oc and the hydroxyl hydrogen Hh, which were involved in the most important of the acid-acid bonds, are also involved in a strong bond with water molecules. If we examine the position of the first near neighbour peaks in these RDFs, we immediately notice that: (a) the Ow···Hw peak is at the same position (1.75 Å, marked by a vertical line) of the Oc···Hh peak; (b) the Oc···Hw peak for formic acid is shorter than this distance (1.65 Å), while it is longer (1.85 Å) for acetic acid; (c) the Hh···Ow peak for acetic acid is shorter than this distance (1.65 Å), while it is longer (1.85 Å) for formic acid; (d) The Ow···Hw peak is slightly longer (1.8 Å) in pure water than it

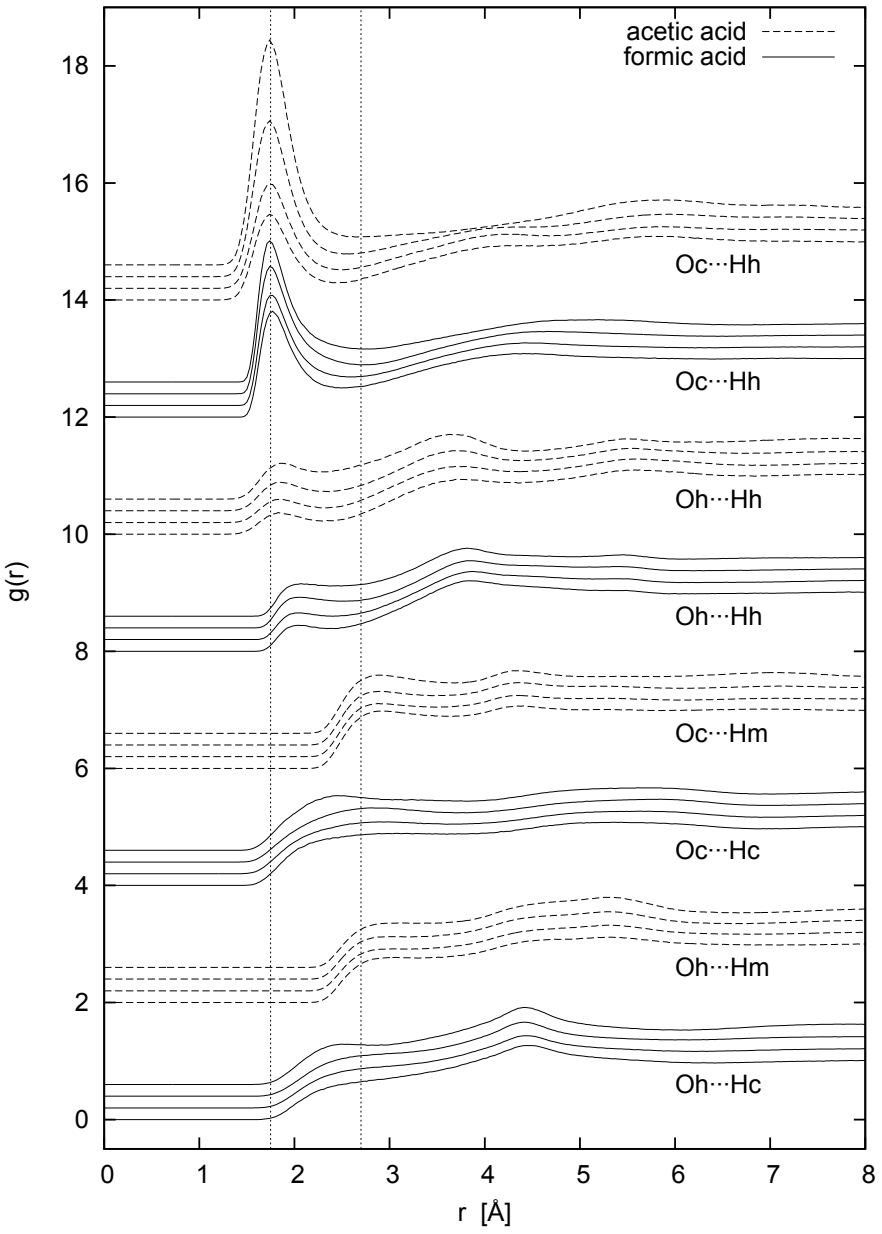

Figure 3: Radial distribution functions (RDFs) relative to oxygen-hydrogen bonds between acid molecules, with formic acid in a continuous line and acetic acid in a dashed line. The plots are shifted arbitrarily. The three concentrations examined in this paper are plotted together with the pure acid results already reported in [17]. The pure acid is the top line of each group of four, followed by 70% and 50%, with 30% at the bottom. Two notable peak positions have been highlighted by a vertical line, at 1.75Å and at 2.7Å, to facilitate comparison across the other RDFs figures, more details in the text.

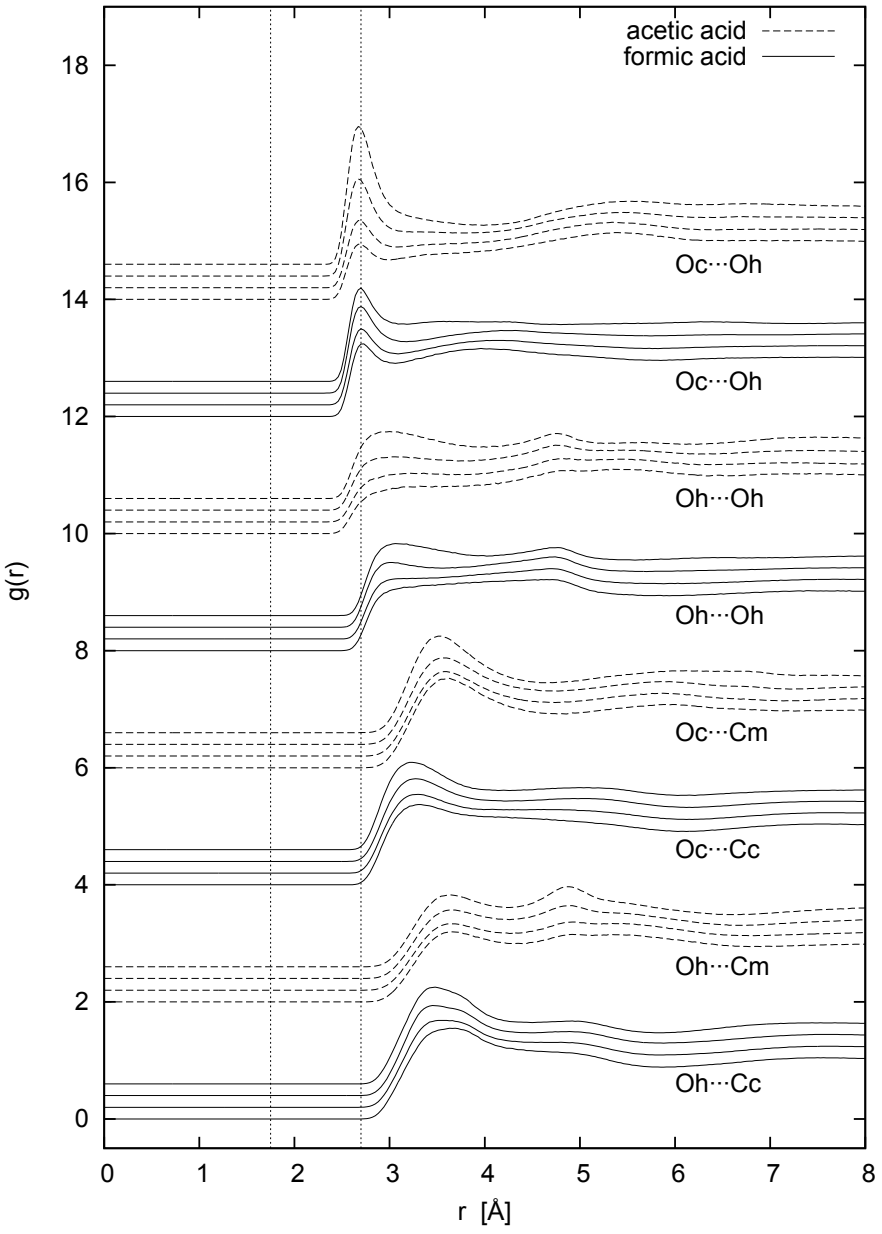

Figure 4: Radial distribution functions relative to oxygen-oxygen and oxygen-carbon bonds between acid molecules. See 3 for more details.

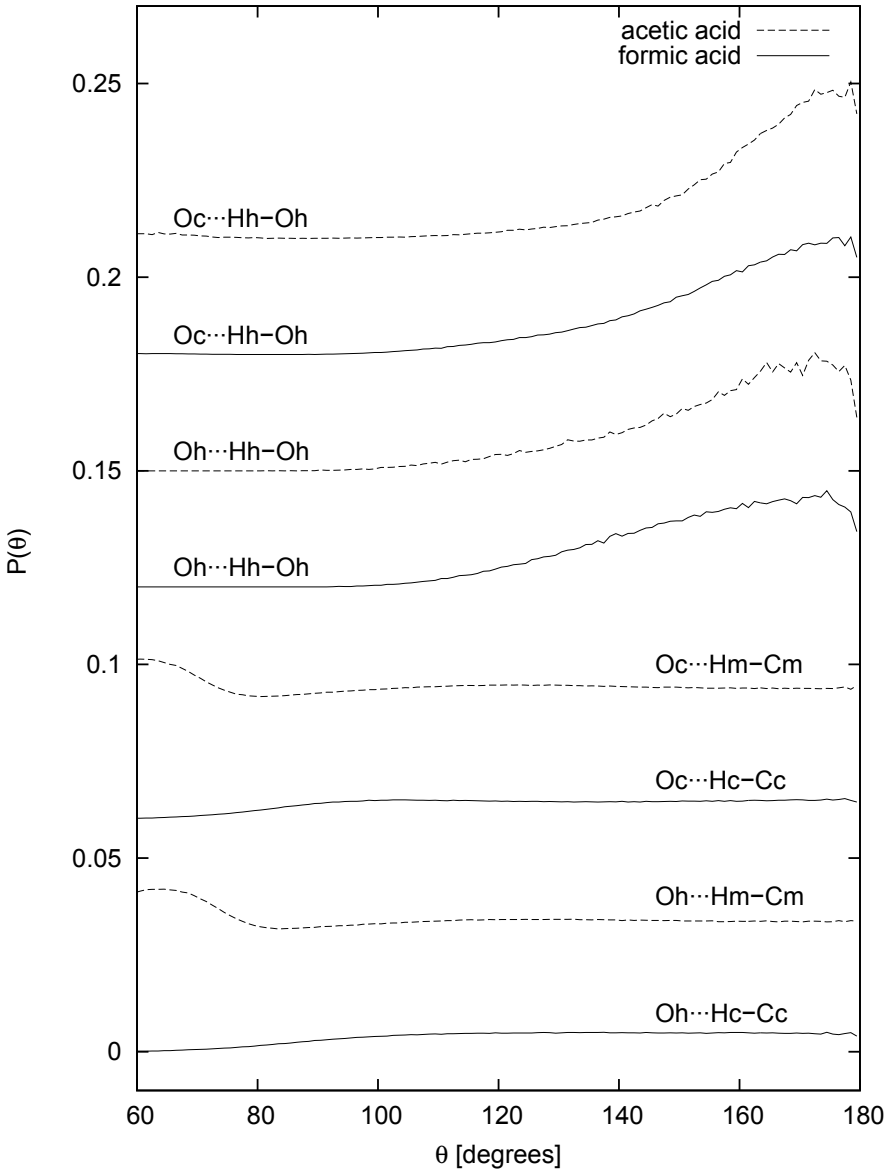

Figure 5: Angular distribution functions for the hydrogen bonds between acid molecules, with formic acid in a continuous line and acetic acid in a dashed line. The plots are shifted arbitrarily. To avoid redundancy, only the 30% concentration has been shown. Notice that the abscissae axis is limited to 60°-180°.

Table 5: Coordination number and chosen radial limit for its calculation for formic and acetic acid. The coordination number is calculated numerically as the number of atoms β to be found within a certain radius from atom α.(second part)

bond	r_{max} [Å]	a.a. 70%	a.a. 50%	a.a. 30%
Oc···Hm	3.5	3.1 ± 1.6	2.7 ± 1.6	2.1 ± 1.5
Hm···Oc	3.5	1.0 ± 0.8	0.9 ± 0.8	0.7 ± 0.7
Oc···Hh	2.5	0.6 ± 0.5	0.4 ± 0.5	0.2 ± 0.4
Hh···Oc	2.5	0.6 ± 0.5	0.4 ± 0.5	0.2 ± 0.4
Oc···Hw	2.5	0.5 ± 0.6	0.8 ± 0.7	1.1 ± 0.7
Hw···Oc	2.5	0.5 ± 0.5	0.4 ± 0.5	0.2 ± 0.4
Oh···Hm	3.5	2.5 ± 1.5	2.2 ± 1.5	1.7 ± 1.4
Hm···Oh	3.5	0.8 ± 0.8	0.7 ± 0.7	0.6 ± 0.7
Oh···Hh	2.5	0.2 ± 0.4	0.1 ± 0.3	0.1 ± 0.2
Hh···Oh	2.5	0.2 ± 0.4	0.1 ± 0.3	0.1 ± 0.2
Oh···Hw	2.4	0.2 ± 0.4	0.3 ± 0.5	0.4 ± 0.5
Hw···Oh	2.4	0.2 ± 0.4	0.2 ± 0.4	0.1 ± 0.3
Ow···Hm	3.5	3.2 ± 1.6	2.8 ± 1.6	1.9 ± 1.5
Hm···Ow	3.5	0.5 ± 0.7	0.9 ± 0.9	1.5 ± 1.2
Ow···Hh	2.5	0.8 ± 0.5	0.6 ± 0.6	0.3 ± 0.5
Hh···Ow	2.5	0.4 ± 0.5	0.6 ± 0.5	0.8 ± 0.4
Ow···Hw	2.4	0.4 ± 0.6	0.8 ± 0.7	1.1 ± 0.8
Hw···Ow	2.4	0.2 ± 0.4	0.4 ± 0.5	0.6 ± 0.5

is in these solutions. Therefore the information that we may draw from this evidence is that the bond structure of the water molecules is not heavily altered even when their concentration is lower or comparable to that of the acid; the bond is slightly stronger than in pure water, and of length comparable to the acid-acid bonds. Water-water coordination numbers (in table 4) decrease with the water content as expected, presumably because of the reduced coordination at the interfaces. The Oc lone pairs are more attractive to hydrogens in formic acid than in acetic acid, while the Oh-Hh dipole is stronger in acetic acid than in formic acid, as already seen in the case of acid-acid correlations. Interestingly, when reconsidering the main peak in the Oc-Hh RDF, it occurs at the same position for both acids, presumably because the two contributions cancel.

The number of water molecules that form a bond with the hydroxyl hydrogen increases with dilution for both acids (see figure 9), thus confirming the competition element already mentioned. The same argument holds for Oc···Hw coordination numbers. As expected, the three bonds examined so far present a linear arrangement of the respective oxygen-hydrogen···oxygen atoms involved (figure 8). Finally the RDFs involving the carbonyl hydrogen Hc and methyl hydrogen Hm are very similar to their corresponding acid-acid RDFs, with similar consideration following. The trends in the oxygen-oxygen RDFs (figure 8) are a confirmation of the analysis performed starting from the oxygen-hydrogen ones.

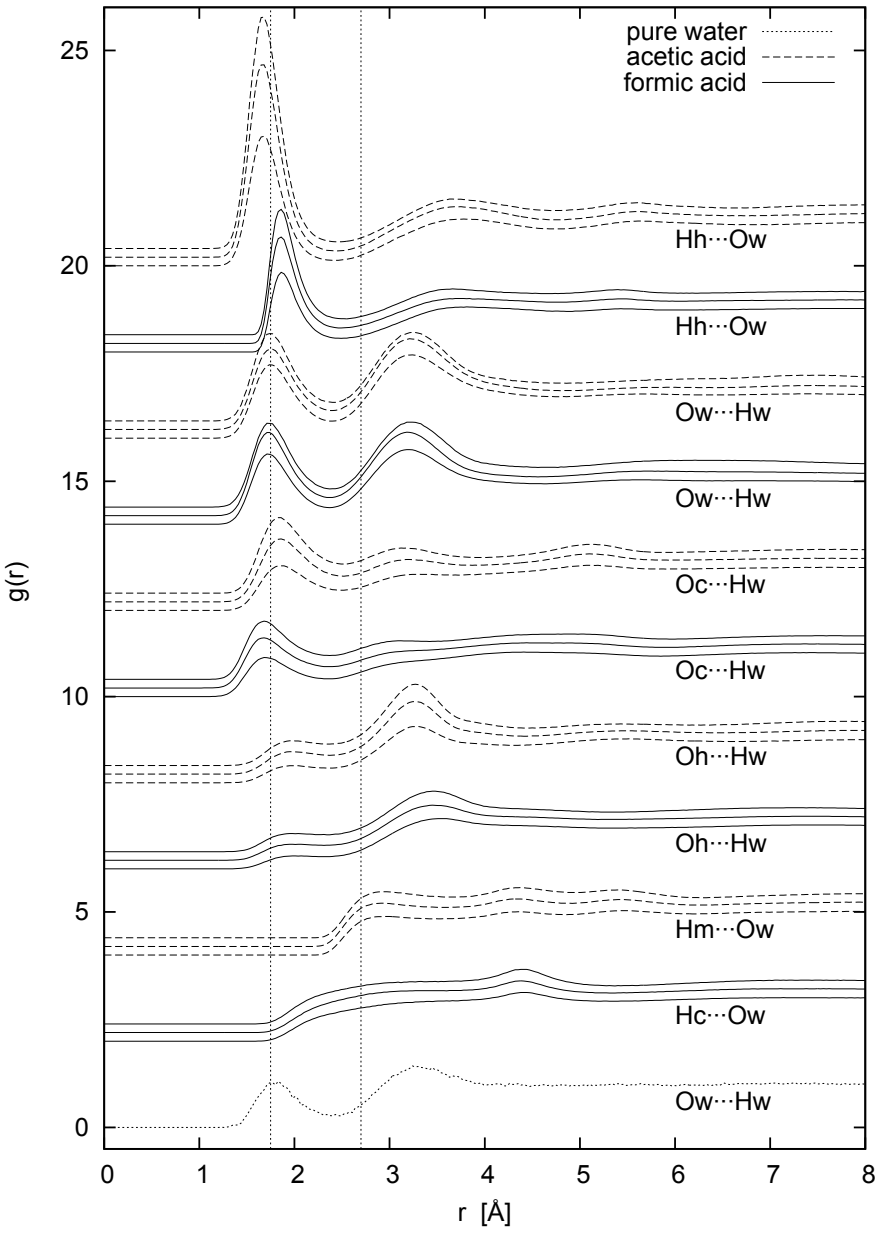

Figure 6: Radial distribution functions relative to oxygen-hydrogen bonds between acid molecules and water molecules, with formic acid in a continuous line and acetic acid in a dashed line. The three concentrations examined in this paper are reported together with the Ow···Hw RDF for pure water (dotted line at the bottom of the figure). The 70% concentration is the top line of each group of three lines, followed by 50%, with 30% at the bottom.

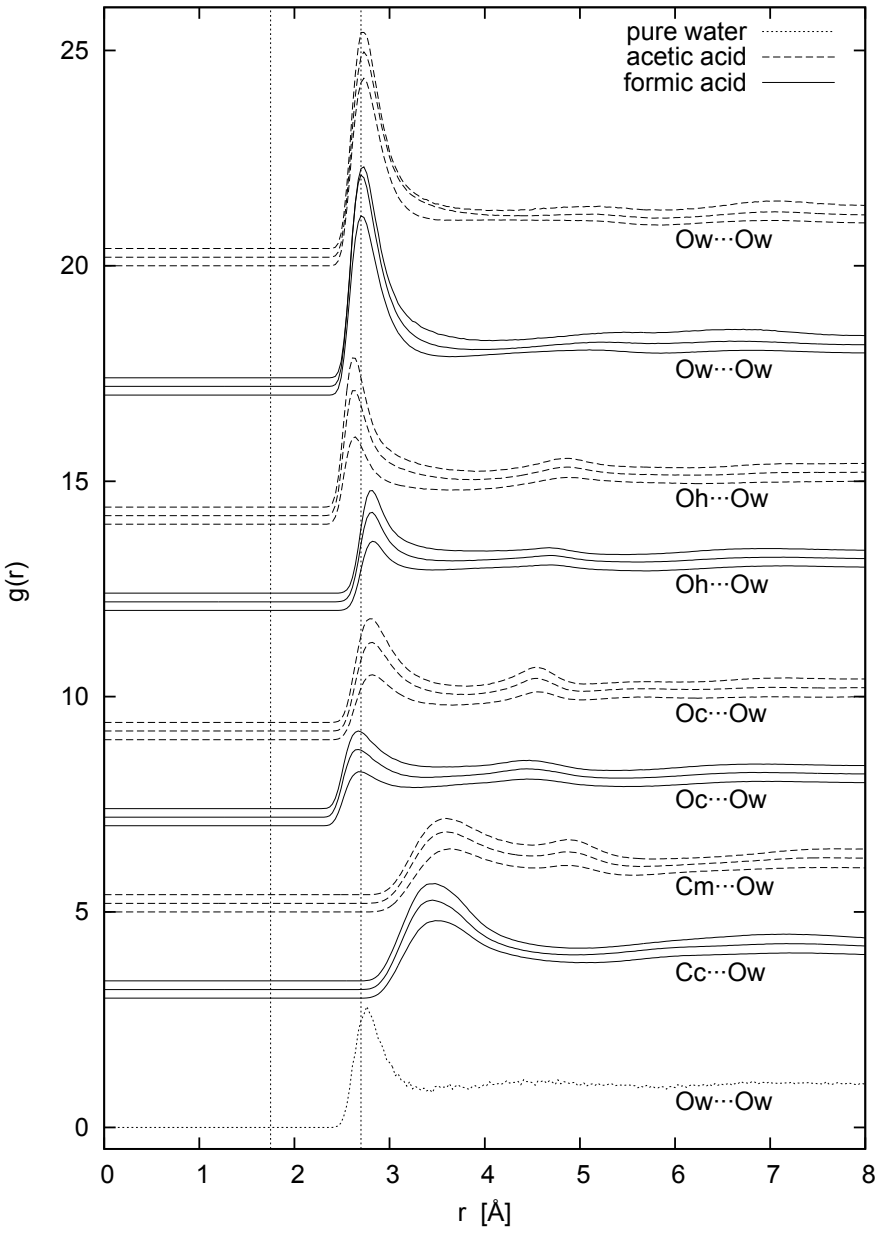

Figure 7: Radial distribution functions relative to oxygen-oxygen and oxygen-carbon bonds between acid molecules and water molecules. The three concentrations examined in this paper are reported together with the Ow···Ow RDF for pure water (dotted line at the bottom of the figure). The 70% concentration is the top line of each group of three lines, followed by 50%, with 30% at the bottom.

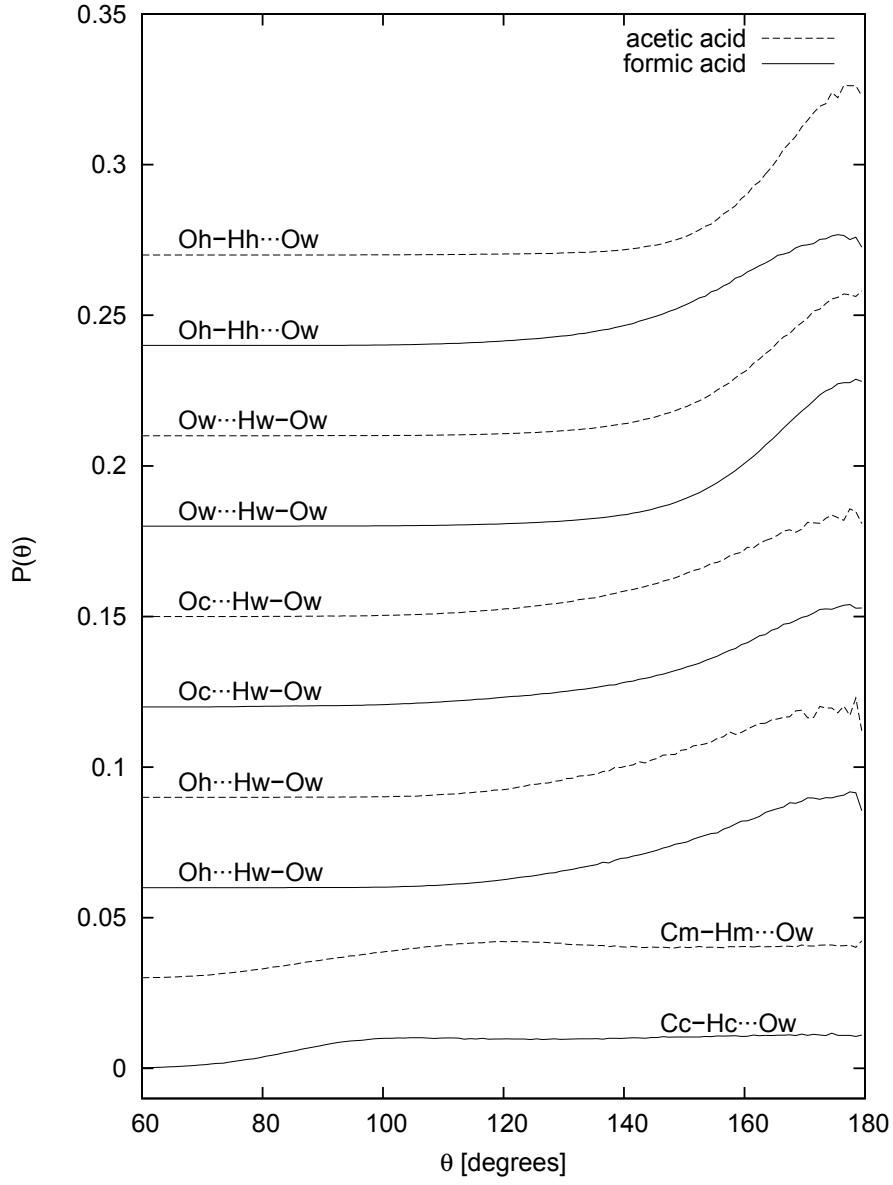

Figure 8: Angular distribution functions for the hydrogen bonds between acid molecules and water molecules, with formic acid in a continuous line and acetic acid in a dashed line. The plots are shifted arbitrarily. To avoid redundancy, only the 30% concentration has been shown. Notice that the abscissae axis is limited to 60°-180°.

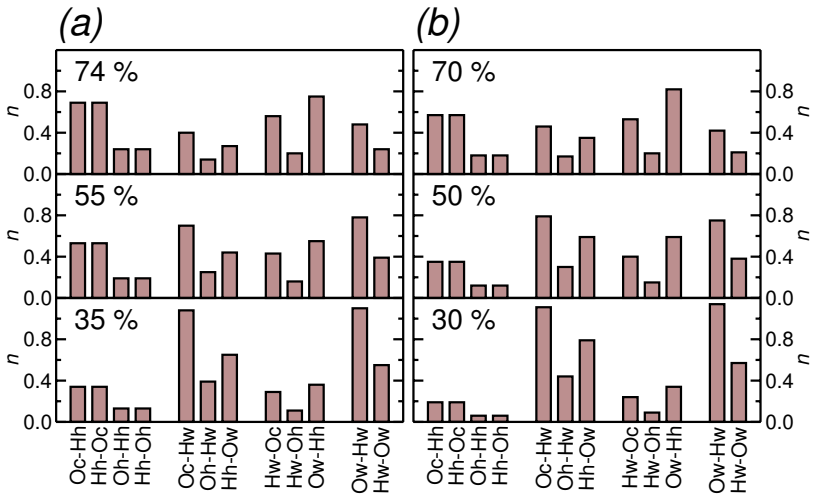

Figure 9: Coordination numbers for (a) formic and (b) acetic acid solutions. Coordination numbers are monotonically increasing or decreasing with concentration in an expected way, but there is a slight increase in the total coordination number for both molecules (see text).

4. Conclusions

The microscopic structure of three solutions of formic acid in water and acetic acid in water have been studied by means of neutron diffraction, aided by H/D substitution[20]. The concentrations studied are approximately 0.7, 0.5 and 0.3 molar fraction. With the help of an EPSR simulation, an ensemble of three-dimensional models of the systems under study have been created. From the computational model, the full set of site-site radial distribution functions (RDFs) has been extracted, as well as coordination numbers, angular distributions and a measure of the connectivity inside each box, called cluster probability.[6]

Among the acid-acid correlations, the most prominent feature is a peak at 1.75 Å in the carbonyl oxygen Oc to hydroxyl hydrogen Hh RDF. The considerable linearity of the Oh-Hh$\cdots$Oc angles, together with the intensity of the peak and the fact that it occurs at a distance comparable (in fact slightly shorter) than the O-H bond in water, indicates the presence of a strong Oc-Hh bond in these solutions.

The peak position is not appreciably modified by the addition of water at any of the concentrations studied so far, while its intensity varies in the case of acetic acid. Together with other evidence, this seems to suggest that the tendency to form an acid-acid bond is more disturbed by the presence of water in the acetic acid than it is in the formic acid case. This is in line with findings from Ref. [4].

The second important feature is in the Oh$\cdots$Hh RDF, which presents a main peak at 2.0 Å for formic acid and at 1.85 Å for acetic acid. The coordination

numbers suggest that it may be not very frequent. Nevertheless, when present, it is close to linear, presumably because of the strong hydroxyl dipole being involved in the bond as in the case of the Oc···Hh just seen. This reflects the fact that the partial charges on the Oh and Hh atoms are slightly bigger (O-H partial charges difference is approximately $0.4e$ greater) for acetic acid than for formic acid. Therefore the ability of the hydroxyl group to form hydrogen bonds is enhanced in acetic acid, and this results in a higher degree of correlation between acid and water molecules.

The most prominent features in the acid-water correlation functions are in the Hh···Ow, Ow···Hw and Oc···Hw RDFs. Is it important to notice that the carbonyl oxygen Oc and the hydroxyl hydrogen Hh, which were involved in the most important acid-acid bonds, are also involved in a strong bond with water molecules. Overall both acid molecules and water molecules have an increase in their total coordination number, when more water molecules are added, a result in agreement with the findings of [18]. It is therefore possible to state that cooperative effects intervene in making hydrated acid molecules "stickier". The quantification of such effects is beyond the capabilities of the present technique. Nevertheless, this finding has important consequences for the physical chemistry of aerosol particles and it would deserve closer inspection. The interpretation of structural data also presents some limitations, for example when trying to determine the relative importance of different hydrogen bond types, based solely on geometrical considerations (see [17]).

From the theoretical point of view, the availability of such good quality structural data on the liquid states is of great importance for the understanding of spectroscopic experiments and for benchmarking both classical molecular dynamics and ab initio simulations. The availability of these data may have a broader impact, as formic acid is often regarded as a test bench for the simulation of hydrogen bonded systems alternative to water.[31] The information collected through experimental and simulation studies will provide a means to develop more realistic and robust models of the formation of atmospheric aerosols and of the their involvement in cloud evolution processes.

Acknowledgements

S. Soffientini wishes to thank Milano-Bicocca University for granting him a *Premio di studio per lo svolgimento della tesi di laurea magistrale all'estero nell'ambito del programma Extra Plus (con il contributo della Fondazione Cariplo) nell'anno accademico 2010/2011*. He wishes to thank STFC Rutherford Appleton Laboratory for hosting him through the subscription of a Co-tutorship bilateral agreement with University of Milano-Bicocca. S. Imberti wishes to acknowledge the ISIS Facility Access Panels from assigning beam-time and expenses funding on experiment proposal RB910589. She also wishes to thank D.T. Bowron for critical reading of the manuscript. All authors wish to thank Prof G. Gorini for his support to this work.

References

[1] U. Lohmann, J. Feichter, Global indirect aerosol effects: a review, Atmospheric Chemistry and Physics 5 (2005) 715–737.

[2] D. A. Hegg, M. B. Baker, Nucleation in the atmosphere, Reports on Progress in Physics 72 (2009) 056801.

[3] B. Zobrist, C. Marcolli, D. A. Pedernera, T. Koop, Do atmospheric aerosols form glasses?, Atmospheric Chemistry and Physics Discussions 8 (2008) 9263–9321.

[4] M. Gadermann, D. Vollmar, R. Signorell, Infrared spectroscopy of acetic acid and formic acid aerosols: pure and compound acid/ice particles, Phys. Chem. Chem. Phys. 9 (2007) 4444–51.

[5] T. Koop, J. Bookhold, M. Shiraiwa, U. Pöschl, Glass transition and phase state of organic compounds: dependency on molecular properties and implications for secondary organic aerosols in the atmosphere., Physical chemistry chemical physics : PCCP 13 (2011) 19238–55.

[6] A. K. Soper, Empirical Potential Structure Refinement - EPSRshell: a user's guide. Version 18, Technical Report RAL-TR-2011-012, Rutherford Appleton Laboratory Report, 2011.

[7] L. Turi, J. J. Dannenberg, Molecular Orbital Study of Crystalline Acetic Acid. 2. Aggregates in One, Two, and Three Dimensions, Journal of the American Chemical Society 116 (1994) 8714–8721.

[8] G. H. Kwei, R. F. Curl, Microwave Spectrum of O18 Formic Acid and Structure of Formic Acid, The Journal of Chemical Physics 32 (1960) 1592.

[9] R. J. Bartholomew, D. E. Irish, Raman spectral study of neat formic acid and aqueous and organic solutions of formic acid, Journal of Raman Spectroscopy 30 (1999) 325–334.

[10] K. Kosugi, Low-frequency Raman spectra of crystalline and liquid acetic acid and its mixtures with water. Is the liquid dominated by hydrogen-bonded cyclic dimers?, Chemical Physics Letters 291 (1998) 253–261.

[11] Z. Zhou, Y. Shi, X. Zhou, Theoretical Studies on the Hydrogen Bonding Interaction of Complexes of Formic Acid with Water, The Journal of Physical Chemistry A 108 (2004) 813–822.

[12] S. Aloisio, P. E. Hintze, V. Vaida, The Hydration of Formic Acid, The Journal of Physical Chemistry A 106 (2002) 363–370.

[13] D. Priem, T.-K. Ha, A. Bauder, Rotational spectra and structures of three hydrogen-bonded complexes between formic acid and water, The Journal of Chemical Physics 113 (2000) 169.

[14] P. R. Rablen, J. W. Lockman, W. L. Jorgensen, Ab Initio Study of Hydrogen-Bonded Complexes of Small Organic Molecules with Water, The Journal of Physical Chemistry A 102 (1998) 3782–3797.

[15] N. Akiya, P. E. Savage, Role of water in formic acid decomposition, AIChE Journal 44 (1998) 405–415.

[16] R. Chelli, R. Righini, S. Califano, Structure of liquid formic acid investigated by first principle and classical molecular dynamics simulations., The journal of physical chemistry. B 109 (2005) 17006–13.

[17] S. Imberti, D. T. Bowron, Formic and acetic acid aggregation in the liquid state., Journal of physics. Condensed matter : an Institute of Physics journal 22 (2010) 404212.

[18] T. Takamuku, Y. Kyoshoin, H. Noguchi, S. Kusano, T. Yamaguchi, Liquid structure of acetic acid-water and trifluoroacetic acid-water mixtures studied by large-angle X-ray scattering and NMR., The journal of physical chemistry. B 111 (2007) 9270–80.

[19] J.-P. Hansen, I. McDonald, Theory of Simple Liquids, Academic Press, Amsterdam, 2006.

[20] J. L. Finney, A. K. Soper, Solvent structure and perturbations in solutions of chemical and biological importance, Chemical Society Reviews 23 (1994) 1 – 10.

[21] A. K. Soper, GudrunN and GudrunX: programs for correcting raw neutron and X-ray diffraction data to differential scattering cross section - July 2011, Technical Report RAL-TR-2011-013, Rutherford Appleton Laboratory Report, 2011.

[22] V. F. Sears, Neutron scattering lengths and cross sections, Neutron News 3 (1992) 26.

[23] A. K. Soper, E. R. Barney, Extracting the pair distribution function from white-beam X-ray total scattering data, Journal of Applied Crystallography 44 (2011) 714–726.

[24] A. K. Soper, Computer simulation as a tool for the interpretation of total scattering data from glasses and liquids, Molecular Simulation 38 (2012) 1171–1185.

[25] T. Hassinen, M. Peräkylä, New energy terms for reduced protein models implemented in an off-lattice force field, Journal of Computational Chemistry 22 (2001) 1229–1242.

[26] H. J. C. Berendsen, J. R. Grigera, T. P. Straatsma, The missing term in effective pair potentials, J. Phys. Chem. 91 (1987) 6269–6271.

[27] W. L. Jorgensen, D. S. Maxwell, J. Tirado-Rives, Developement and testing of the OPLS All-Atom force field on conformational energetics and properties of organic liquids. - supporting information pages 1- 12, J. Am. Chem. Soc. 118 (1996) 11225 – 11236.

[28] P. Jedlovszky, L. Turi, Role of the CHO Hydrogen Bonds in Liquids: A Monte Carlo Simulation Study of Liquid Formic Acid Using a Newly Developed Pair-Potential, The Journal of Physical Chemistry B 101 (1997) 5429–5436.

[29] P. Jedlovszky, L. Turi, A New Five-Site Pair Potential for Formic Acid in Liquid Simulations, The Journal of Physical Chemistry A 103 (1999) 3796–3796.

[30] E. Arunan, G. R. Desiraju, R. a. Klein, J. Sadlej, S. Scheiner, I. Alkorta, D. C. Clary, R. H. Crabtree, J. J. Dannenberg, P. Hobza, H. G. Kjaergaard, A. C. Legon, B. Mennucci, D. J. Nesbitt, Defining the hydrogen bond: An account (IUPAC Technical Report), Pure and Applied Chemistry 83 (2011) 1619–1636.

[31] M. R. Johnson, H. P. Trommsdorff, Vibrational spectra of crystalline formic and acetic acid isotopologues by inelastic neutron scattering and numerical simulations, Chemical Physics 355 (2009) 118–122.